Cooling load and noise characterization modeling for photovoltaic driven building integrated thermoelectric cooling devices

Himanshu Dehra

Egis India Consulting Engineers Pvt. Ltd., Egis Tower, Plot # 66, Sector 32, Gurugram 122001 (Haryana), India

Abstract. Photovoltaic driven thermoelectric cooling devices are investigated for installation in a modular outdoor test-room. Because of Peltier effect in a thermoelectric cooling (TEC), heating and cooling is achieved by applying a voltage difference across the thermoelectric module. Theoretical design modeling of cooling load and noise characterization of building integrated Thermoelectric (TEC) Devices is analyzed. System design of photovoltaic driven TEC devices is investigated with varying fresh outdoor ventilation rates. Building integrated design of TEC devices inside ceiling suspended duct along with TEC devices mounted on wall driven by rooftop and active façade photovoltaic devices is considered in the analysis. In this way, two-stage dehumidification is achieved by two different sets of TEC devices. The investigation is conducted for effect of voltage, air flow rate and height of fin heat transfer surface. Expressions along with results for noise characterization in photovoltaic driven building integrated TEC devices are also provided.

1 Introduction

Thermoelectric module is a solid-state energy conversion device made up of thermocouples, which are wired in series electrical circuit and parallel thermal junctions. A thermocouple consists of N-type and P-type semi-conductor elements, to generate thermoelectric cooling (viz., Peltier – Seebeck effect) when a voltage difference in appropriate direction is applied through the connected circuit. The temperature of the cold junction gradually decreases with heat transfer mechanism from environment to cold junction at a lower temperature. This heat transfer mechanism takes place with passing of transport electrons from a low energy level inside the P-type thermocouple element to a high energy level inside the N-type thermocouple element through the cold junction. Simultaneously, transport electrons transmit absorbed heat to hot junction at a higher temperature. This extra generated heat is dissipated to heat sink, whereas transport electrons return to a lower energy level in the P-type semiconductor element, viz., the Peltier effect takes place (see Figure 1).

The design of thermoelectric cooling system is based on temperature difference across the hot and cold sides of the TEC module and the required cooling capacity. In this paper energy balance model and noise characterization is presented for evaluating system design of a prototype thermoelectric cooling – photovoltaic (TEC-PV) device. The prototype consists of an integrated design with ceiling suspended, wall mounted, rooftop and active façade TEC-PV devices [1].
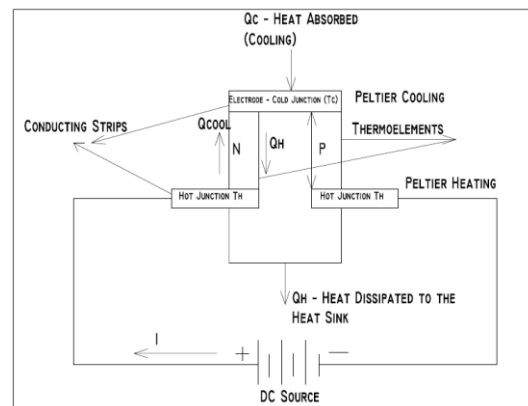

Figure 1: Principle of Thermoelectric Cooling

2 Energy Balance Model

The total energy efficiency of photovoltaic driven thermoelectric cooling devices can be increased with enhancement of photovoltaic system efficiency and with the use of thermoelectric materials with better performance. The COP of thermoelectric air conditioning devices powered through photovoltaic modules is typically not higher than 0.6 [2]. With consideration of photovoltaic system efficiency η_{pv}, the total energy efficiency of the system is given by the product of η_{pv} and COP. Mathematically it is written as:

$$E_{TEC-PV} = \eta_{pv} \times COP \quad (1)$$

The values of $E_{TEC\text{-}PV}$ are typically lower than 6%.

---

* Himanshu Dehra (Corresponding author): anshu_dehra@hotmail.com

Commercial thermoelectric materials are alloys such as Bi_2Te_3, $PbTe$, $SiGe$ and $CoSb_3$. Bi_2Te_3 is the most commonly used thermoelectric material. The commercially available thermoelectric materials have highest ZT values around 1.0.

For a particular thermoelectric module with fixed hot/cold side temperatures, the maximum COP at optimum current is given by [3]:

$$COP_{max, cool} = \frac{T_c}{T_h - T_c} \cdot \frac{\sqrt{1 + ZT_m} - \frac{T_h}{T_c}}{\sqrt{1 + ZT_m} + 1} \quad (2)$$

Where, ZT_m is the figure-of-merit for thermoelectric material at mean hot and cold side temperature T_m. In calculation of COP, a mean temperature between the hot and cold junction temperatures (with fixed hot side temperature of 300 K with $ZT_m = 1$) of the thermoelectric module (TEM) is used.

A steady state energy balance model of thermoelectric cooling is used for energy performance assessment.

$$COP_{cooling} = \frac{Q_c}{P} \quad (3)$$

In order to investigate the operating energy consumption in summer, a thermoelectric cooling-photovoltaic (TEC-PV) device is simulated for building data as per Table 1, representing sunny, hot and humid outdoor air condition. Properties of TEC-PV device is provided in Table 2.

Table 1: Building Data

Outdoor Air Condition	Sunny, Hot and Humid (DBT: 33-35 °C, RH: 75%)		
Floor Area	9 m²		
Room Volume	27 m³		
U-value of Exterior Wall	0.44 W/m²K		
U-value of Roof	0.126 W/m²K		
Window to wall ratio	0.3		
Lighting Power Density	0.6 W/ft²		
Infiltration	0.3 ACH		
Operation Schedule	07:00 to 17:00 hours		
Indoor Air Condition	Dry Bulb Temperature (DBT): 23 °C, RH: 55%		
Room Sensible Heat Factor	0.95	0.9	0.8	0.7
Ventilation Rate	20 m³/h	40 m³/h	90m³/h	120 m³/h
Peak sensible cooling load	1 kW			
Peak latent cooling load	0.05 kW	0.12 kW	0.28 kW	0.48 kW

Table 2: Thermoelectric Cooling (TEC)-Photovoltaic (TEC-PV) Device Properties

TEC Module	TEC1-12710	Photovoltaic Module	
Operational Voltage	12 V DC	Total Power Required	1.8 kW
Current Max	10.5 Amp	Area required	18 m²
Voltage Max	15.2 V	Roof Area	9 m²
Power Max	85 W	South façade area	9 m²
Nominal Power	60 W	Nominal Power	300 W
Thermocouples	127	Number of PV modules	8
Dimensions	40 X 40 X 3.5 mm	On roof	4
Total Number of TEC Modules	30	On façade	4
Placement Position	Inside Ceiling Duct	Wall mounted	Battery Backup	10.8 kWh
TEC Modules	10	20	Battery @ 12 V DC	900 AH

2.1. Thermoelectric Dehumidification

The room sensible heat factor (RSHF) is defined as the ratio of sensible cooling load to total cooling load (Equation 4).

$$RSHF = \frac{Q_{sen}}{Q_{sen} + Q_{lat}} \quad (4)$$

Relative humidity is a key control parameter for thermal comfort inside a room. The performance of a thermoelectric cooling device depends mainly on optimal positioning and layout of heat exchange & transfer surfaces.

The total heat transfer rate (Q_c) of the fin heat exchanger on the cold side of the thermoelectric module (TEM) is given by [4]:

$$Q_c = h_c \cdot A_c \cdot (t_r - t_c) + m_w \cdot H_c \quad (5)$$

Where, h_c is the coefficient of convective heat transfer (W/m²K), A_c is the heat transfer area (m²), t_r is the room temperature (°C), t_c is average temperature of cold fins (°C) and H_c is the latent heat of condensation (J/kg-K). The dehumidifying rate (m_w, kg/s) is calculated as [5]:

$$m_w = \frac{m_a \cdot (\phi_1 - \phi_2)}{T_{sec}} \quad (6)$$

Where, m_a is the mass of the wet air inside the room (kg), T_{sec} is the dehumidifying period (sec), Φ_1 and Φ_2 are the relative humidity before and after dehumidification (%). The convective heat transfer coefficient between adjacent fins and room air is [6]:

$$h_c = 0.517 \cdot \frac{k_{air}}{H} \cdot Ra^{0.25} \quad (7)$$

2 Design Considerations for thermoelectric Cooling – Photovoltaic (TEC-PV) Devices

Building integration parameters: Thermoelectric cooling (TEC) devices can be fixed in a building on wall and ceiling as radiant cooling panels. Due consideration should be given for placing thermoelectric modules with or without heat sinks. Heat sinks can be placed towards building interior zone and towards exterior zone. The thermoelectric modules can be placed on a cut section of a wall, with provision of cooling the hot side heat sink. The thermoelectric cooling devices can also be fixed on

a window or a skylight. Proper protection has to be ensured from air infiltration and direct solar radiation for TEC devices fixed on windows and skylights. The mode of operation for winter can be reversed by changing the direction of current of thermoelectric modules. TEC devices can also be fixed inside air supply ventilation ducts. Buildings requiring cooling and heating with dual duct ventilation system are good choice for using thermoelectric devices inside ducts.

Thermoelectric module (TEM) system design: It depends on thermoelement length, number of thermocouple legs, cross sectional area, slenderness ratio. Both COP and cooling capacity of TEC devices are dependent on thermoelement length. Keeping cross sectional area constant, larger length of thermoelectric element achieves greater COP, while shorter length thermoelectric element achieves larger cooling capacity. Commercially available thermoelectric modules have thermoelement length in the range from 1 mm to 2.5 mm. Cooling power capacity increases with decreasing the ratio of thermoelement length to cross sectional area.

Thermoelectric cooling (TEC) system design: It depends on cooling system thermal design, heat sinks' geometry, heat transfer area, heat transfer coefficients of hot and cold side heat sinks, thermal and electrical contact resistances, fins placement and design, heat sinks integrated with thermosyphon, heat transfer fluids, phase change materials [7]. Thermal contact resistance at the interface layer of thermocouple legs are critical for its cooling capacity and COP. Because of this reason, it is not essential that increase in ZT of thermoelectric material will increase ZT of a thermocouple leg because of the presence of interface layer. The performance and efficiency of heat sinks at hot and cold side effects the cooling COP. Air cooled heat sink (forced convection with fan, example thermal resistances of 0.54-0.66 K/W, water cooled heat sink (thermal resistance of 0.108 K/W, and heat sink integrated with heat pipe (thermal resistance 0.11 W/K are most commonly used techniques.

Photovoltaic (PV) power system design: The most conventional way is to install PV panels on rooftop and façade of a building with thermoelectric cooling (TEC) devices. In this way, excess power can also be stored in a battery system. In case of non-availability of solar PV power, power can be fed directly from the battery backup. Active façade ventilation can be integrated with TEM and PV devices [8]. For heating requirements during winter season, these active façade elements can supplement with heating from TEM and façade integrated PV ventilated devices.

Performance & operational parameters optimization: It depends on electric current input, coolants, cooling methods of hot side heat sink, mass flow rate, ventilation requirements. Performance indicators are COP and energy efficiency of devices and systems.

The system design consists of: i) outdoor fresh air ventilation; ii) thermoelectric cooling (TEC); iii) building integration; iv) photovoltaic power generation; and v) exhaust air ventilation.

Operation: The outdoor fresh air is cooled down and dehumidified as it flows over a heat sink/exchanger attached to thermoelectric cooling (TEC) module. The cool air enters the indoor environment which is to be maintained at 23 °C and 55% RH. The stale air is taken out through ducted exhaust air ventilation system. The exhaust air also cools down the heat sink/exchanger attached to hot side of thermoelectric module (TEM). The outdoor fresh air is introduced into the single zone building air volume at varying rates as mentioned in Table 2. Four DC fans are used to provide power for forced airflow. Two of them are installed on supply fresh air side and other two are installed on exhaust air side. The input power for each fan is 1.5 W with airflow rate at 60 m^3 h^{-1}. The maximum fresh air supply in the room is 120 m^3 h^{-1} at full capacity. The outside fresh air is at 33°C and 75% RH. Eight solar PV modules of 300 W each are used to power thirty TEC modules of 60 W each and four DC fans of 1.5 W each. Four solar PV modules are placed on south façade while other four are fixed on roof top. The maximum sensible cooling load in the building zone is 1 kW while maximum latent load varies up to 0.48 kW.

Principle: There is two-stage cooling. 1st stage inside fresh air supply duct through TEC modules fixed inside air supply duct; 2nd stage-Inside the room through TEC modules fixed on inner wall. Extra cooling is achieved inside the room through TEC modules on façade.

Two-stage Dehumidification (Condensation): Depending on dew point of the air, cooling dehumidification and iso-thermal dehumidification can take place on fins inside cooling duct and on wall with TEC modules. The schematic of a building zone with two stage cooling through TEC modules by means of supply duct and wall mounted TEC modules with solar PV façade exhaust duct is illustrated in Figure 2 a. The performance characteristics with voltage variation of analysed TEC1-12710 modules in TEC calculator is provided in Figure 2 b. The variation in theoretical values of COP (cooling) and temperature (cold) for ZT_m=1 is provided in Figure 3 a. The variation in theoretical values of cooling capacity with temperature difference is provided in Figure 3 b. The variation of theoretical heat transfer coefficient with height of heat transfer surface (fins) is provided in Figure 4 a. The theoretical variation of cooling capacity load served inside room with height of heat transfer surface (fins) is provided in Figure 4 b. All the results are based on theoretical values irrespective of actual performance values of the prototype TEC-PV device.

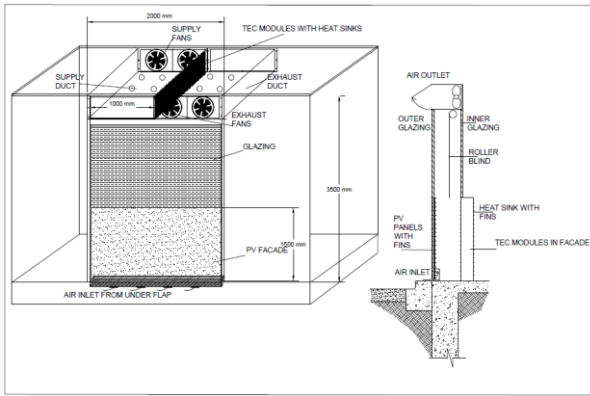# 3 System Design of Thermoelectric Cooling-Photovoltaic (TEC-PV) Device

Figure 2a: Schematic of a building room zone with TEC modules and PV ventilated façade
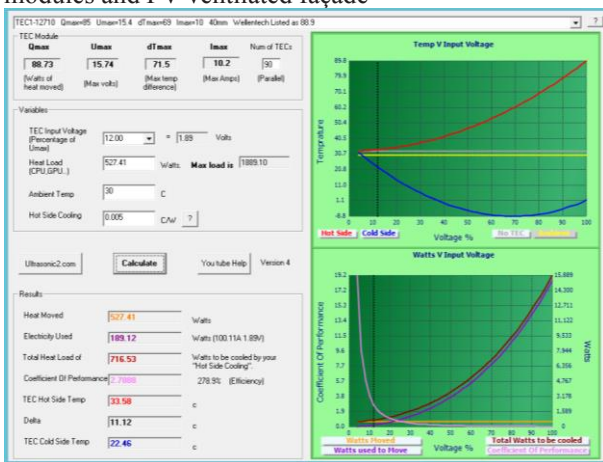

Figure 2b: Performance characteristics of TEC1-12710 module with voltage variation analysed in TEC calculator
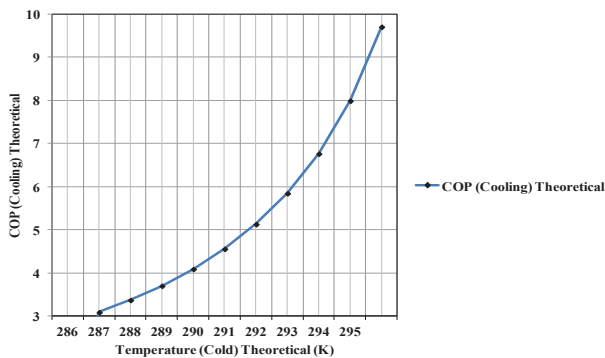

Figure 3a: Variation in theoretical values of COP (Cooling) and Temperature (Cold) for $ZT_m=1$;
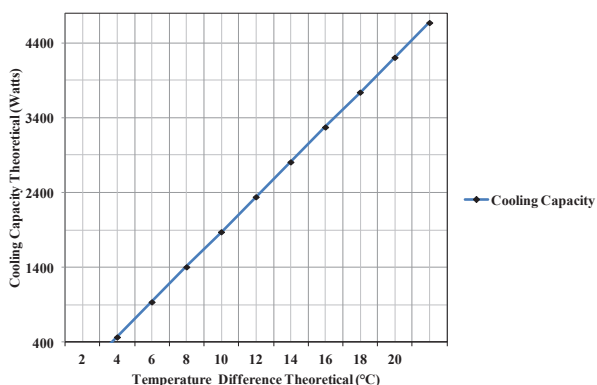

Figure 3b: Variation in theoretical values of cooling capacity with temperature difference
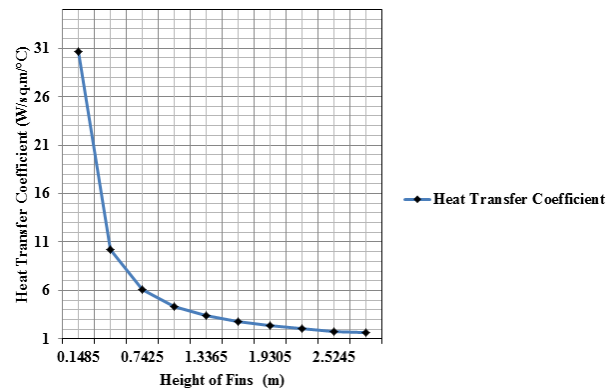

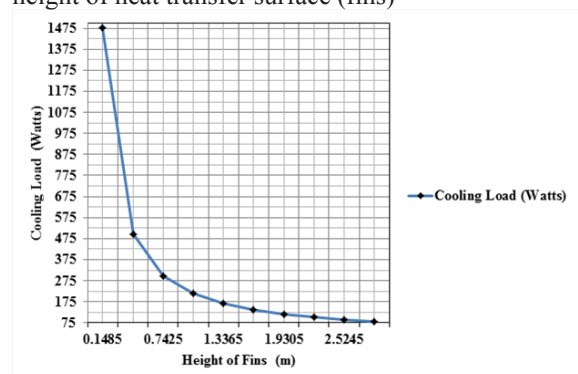Figure 4a) Variation of heat transfer coefficient with height of heat transfer surface (fins)

Figure 4b) Variation of cooling capacity load served inside room with height of heat transfer surface (fins)

4 Noise Characterization

A unified theory for stresses and oscillations is proposed by the author [9]. The following standard measurement equations are derived and adopted from the standard definitions for sources of noise interference [10, 11, 12, 13, 14, 15].

Noise of Sol: For a pack of solar energy wave, the multiplication of solar power storage and the velocity of light gives solar power intensity I. On taking logarithm of two intensities of solar power, I_1 and I_2, provides intensity difference. It is mathematically expressed as:

$$Sol = \log(I_1)(I_2)^{-1} \qquad (8)$$

Whereas logarithmic unit ratio for noise of sol is expressed as *Sol*. The oncisol (oS) is more convenient for solar power systems. The mathematical expression by the following equality gives an oncisol (oS), which is $1/11$th unit of a *Sol*:

$$oS = \pm 11\log(I_1)(I_2)^{-1} \qquad (9)$$

Noise of Therm: For a pack of heat energy wave, the multiplication of total power storage and the velocity of light gives heat power intensity I. The pack of solar energy wave and heat energy wave (for same intensity I), have same energy areas, therefore their units of noise are same as *Sol*.

Noise of Scattering: For a pack of fluid energy wave, the multiplication of total power storage and the velocity of fluid gives fluid power intensity I. On taking logarithm of two intensities of fluid power, I_1 and I_2, provides intensity difference. It is mathematically expressed as:

$$Sip = \log(I_1)(I_2)^{-1} \qquad (10)$$

Whereas, logarithmic unit ratio for noise of scattering is *Sip*. The oncisip (oS) is more convenient for fluid power systems.

The mathematical expression by the following equality gives an oncisip (oS), which is $1/11^{th}$ unit of a *Sip*:

$$oS = \pm 11 \log(I_1)(I_2)^{-1} \qquad (11)$$

For energy area determination for a fluid wave, the water with a specific gravity of 1.0, is the standard fluid considered with power of ± 1 Wm^{-2} for a reference intensity I_2.

Noise of Elasticity: For a pack of sound energy wave, the product of total power storage and the velocity of sound gives sound power intensity I. On taking logarithm of two intensities of sound power, I_1 and I_2, provides intensity difference. It is mathematically expressed as:

$$Bel = \log(I_1)(I_2)^{-1} \qquad (12)$$

Whereas, logarithmic unit ratio for noise of elasticity is *Bel*. The oncibel (oB) is more convenient for sound power systems. The mathematical expression by the following equality gives an oncibel (oB), which is $1/11^{th}$ unit of a *Bel*:

$$oB = \pm 11 \log(I_1)(I_2)^{-1} \qquad (13)$$

There are following elaborative points on choosing an *onci* as $1/11^{th}$ unit of noise [15, 16]:

i) Reference value used for I_2 is -1 W m^{-2} on positive scale of noise and 1 W m^{-2} on negative scale of noise. In a power cycle, all types of wave form one positive power cycle and one negative power cycle [9]. Positive scale of noise has 10 positive units and one negative unit. Whereas, negative scale of noise has 1 positive unit and 10 negative units;

ii) Each unit of sol, sip and bel is divided into 11 parts, 1 part is $1/11^{th}$ unit of noise;

iii) The base of logarithm used in noise measurement equations is 11;

iv) Reference value of I_2 is -1 W m^{-2} with I_1 on positive scale of noise, should be taken with negative noise measurement expression (see Eqs 9, 11 and 13), therefore it gives positive values of noise;

v) Reference value of I_2 is 1 W m^{-2} with I_1 on negative scale of noise, should be taken with positive noise measurement expression (see Eqs 9, 11 and 13), therefore it gives negative values of noise.

The choosing of *onci* in noise units is done so as to have separate market product & system of noise scales and their units distinguished from prevailing *decibel* units (which has its limitations) in the International System of Units. More discussions on energy conversion, noise characterization theory and choice of noise scales and its units are presented in many papers by the author [15, 16]. Tables 3, 4, 5 and 6 have presented sensitivity analysis and noise characterization values for the exterior duct based on mass flow rate, solar irradiation and size of duct. Appendix has provided noise calculation charts.

Table 3. Temperature difference and noise of sol with solar irradiation (air velocity: 0.75 ms^{-1})

Solar irradiation (Wm^{-2})	Air Temperature Difference (ΔT) °C	Noise of Sol oS (oncisol)
450	15.50	28
550	18.90	28.93
650	22.40	29.7
750	25.90	30.36
850	29.40	30.91

Table 4. Temperature difference and noise of scattering with air velocity (S = 650 Wm^{-2})

Air velocity (ms^{-1})	Fluid Power (Wm^{-2})	Air Temperature Difference (ΔT) °C	Noise of Scattering oS (oncisip)
1.35	47.62	15.28	17.72
1.05	37.0	18.22	16.50
0.75	26.45	22.40	15.02
0.45	15.87	28.15	12.65
0.15	05.29	29.80	07.64

Table 5. Mass flow rate and noise of therm with (ΔT)

(ΔT) °C	Mass flow rate (Kg s^{-1})	Thermal Power (Wm^{-2})	Noise of Therm oS (oncisol)	(ΔT) °C	Mass flow rate (Kg s^{-1})	Thermal Power (Wm^{-2})	Noise of therm oS (oncisol)
15.50	0.01376	71.09	19.56	15.28	0.0231	117.65	21.868
18.90	0.01275	80.32	20.11	18.22	0.0171	103.85	21.296
22.40	0.0120	89.6	20.61	22.40	0.0120	89.6	20.614
25.90	0.0115	99.28		28.15	8.1 X 10^{-3}	76.0	19.866
			21.04				
29.40	0.0111	108.8		29.80	6.2 X 10^{-3}	61.59	18.898
			21.50				

Table 6 Noise of elasticity with air particle velocity (Impedance $Z_0 = 413$ N·s·m^{-3} at 20°C)

Air velocity (m·s^{-1})	Fluid Power (W·m^{-2})	Noise of Scattering oS (oncisip)	Sound Pressure (N·m^{-2})	Sound Power Intensity (W·m^{-2})	Noise of Elasticity oB (oncibel)
1.35	47.62	17.72	557.5	752.7	30.36
1.05	37.0	16.50	433.65	455.33	28.05
0.75	26.45	15.02	309.75	232.31	24.97
0.45	15.87	12.65	185.85	83.63	20.24
0.15	05.29	07.64	61.94	09.29	10.12

CONCLUSIONS

Thermoelectric cooling (TEC) is one of the specialized areas in "Thermoelectrics". This paper has presented the summary of energy modeling parameters representing various cooling load performance and noise characteristics of building integrated thermoelectric cooling-photovoltaic (TEC-PV) devices. There is significant growing interest level in thermoelectric cooling (TEC) because of their useful control aspects. This is because TEC modules are readily operated at partial load by changing the electric current. Moreover, there is increase in cooling COP with reduction of cooling power. Air-conditioning of fresh outdoor air for direct indoor use through proper system design of supply air ventilation system and exhaust air ventilation system is another key benefit of thermoelectric cooling (TEC). In addition, photovoltaic (PV) roof-top power generation and photovoltaic (PV) ventilated façade are integrated into the system design, thus making it further sustainably sound in terms of input electricity requirements through green power and active ventilation system for supply and exhaust air. Thermoelectric modules (TEM) offer air-conditioning solutions with flexible electrical loads in contemporary context of smart energy systems for buildings. Finally, the noise interference and characterization equations as per speed of a composite

wave are presented. The noise measurement equations and their units are described depending on their speed of noise interference. Some examples of noise characterization are also presented.

References

1. H. Dehra, 2018 a, Building-Integrated Thermoelectric Cooling-Photovoltaic (TEC-PV) Devices, in book, "Bringing Thermoelectricity into Reality", edited by Patricia Aranguren, IntechOpen, DOI: 10.5772/intechopen.75472, ISBN 978-953-51-6058-8, Chapter 15, 313-330.

2. E. S. Jeong, 2014, A new approach to optimize thermoelectric cooling modules, Cryogenics 59, 38–43.

3. D. Zhao, G. Tan, 2014, A review of thermoelectric cooling: Materials, modeling and applications, Applied Thermal Engineering 66, 15-24.

4. W. Huajun, Q. Chengying, 2010, Experimental study of operation performance of a low power thermoelectric cooling dehumidifier, International Journal of Energy and Environment, Volume 1, Issue 3, 459-466.

5. A. Bejan, G. Tsatusaronis, M. Moran, 1996, Thermal Design and Optimization, Wiley, New York.

6. H. Dehra, 2016 a, A Mathematical Model of a Solar Air Thermosyphon integrated with Building Envelope, International Journal of Thermal Sciences, Vol. 102, 210-227.

7. Y. Yongqiang Luo, L. Zhang, Z. Liu, Y. Wang, F. Meng, J. Wu. 2016, Thermal performance evaluation of an active building integrated photovoltaic thermoelectric wall system, Applied Energy 177, 25–39.

8. H. Dehra, 2007, A Unified Theory for Stresses and Oscillations, Proceedings from CAA Conf. Montréal. 2007, Canada, Canadian Acoustics. September 2007. Vol. 35. No. 3, pp 132-133.

9. H. Dehra, 2008 a, Power Transfer and Inductance in a Star Connected 3-phase RC Circuit Amplifier, Proc. AIChE 2008 Spring Meeting, New Orleans, LA, USA, April 6-10, 2008, session 96a.

10. H. Dehra, 2016 b, A Novel Theory of Psychoacoustics on Noise Sources, Noise Measurements and Noise Filters, INCE Proc. NoiseCon16 Conf., Providence, Rhode Island, USA, 13-15 June, 2016, 933-942.

11. H. Dehra, 2008 b, The Noise Scales and their Units, Proc. CAA Conf., Vancouver 2008, Canada, Canadian Acoustics, Vol. 36 (3) 2008, 78-79.

12. H. Dehra, 2017, A Multi-Parametric PV Solar Wall Device, Proceedings from IEEE International Conference on Power, Control, Signals and Instrumentation Engineering (ICPCSI-2017), Chennai, India on Sep 21-22, 2017, 392-401.

13. H. Dehra, 2018 b, Modeling of Energy Conversion and Noise Characterization in Outdoor Ducts exposed to Solar Radiation, International Conference on Applied Energy (ICAE 2018), Hong Kong, China on Aug 22-25, 2018. 8p.

14. H. Dehra, 2018 c, A Paradigm of Noise Interference in a Wave, Internoise-2018, 47th International Congress and Exposition on Noise Control Engineering, Chicago, Illinois, USA on Aug 26-29, 2018, 451-462.

15. H. Dehra, 2018 d, Acoustic Signal Processing and Noise Characterization Theory via Energy Conversion in a PV Solar Wall Device with Ventilation through a Room, Advances in Science, Technology and Engineering Systems Journal, Vol. 3, No. 4, 2018, pp. 130-172, Special Issue on Multidisciplinary Sciences and Engineering.

16. H. Dehra, 2019, Principles of Energy Conversion and Noise Characterization in Air Ventilation Ducts exposed to Solar Radiation, *Applied Energy*, 242C (15 May 2019), pp. 1320-1345.

Nomenclature

η_{pv}	Photovoltaic system efficiency	K	Thermal Conductance, W/m^2K
COP	Coefficient of performance	I	Electric Current, Amperes
ZT_m	Figure-of-merit for thermoelectric material	N	Number of thermocouple legs
Q_c	Absorbed heat flux, W	L	Thermoelectric leg length, m
Q_h	Released heat flux, W	S	Leg section area, m^2
P	Electric power, W	λ	Thermal conductivity, W/m-K
hc	Coefficient of convective heat transfer (W/m2K),	Qlat	Latent load, W
Ac	Heat transfer area (m2)	Hc	Latent heat of condensation (J/kg-K)
tr	Room temperature (°C)	ma	Mass of the wet air inside the room (kg)
tc	Temperature of cold fins (°C)	Tsec	Dehumidifying period (sec)
$\Phi 1$	Relative humidity before dehumidification (%)	kair	Thermal conductivity of air (W/m-K)
$\Phi 2$	Relative humidity after dehumidification (%)	H	Height of fin (m)

Appendix

Fig. 5 has presented a double-sided hexagonal slide rule with seven edges for noise measurement representing seven sources of noise. Reference value used for I_2 is -1 W m^{-2} on positive scale of noise and 1 W m^{-2} on negative scale of noise. Positive scale of noise has 10 positive units and one negative unit. Whereas, negative scale of noise has 1 positive unit and 10 negative units. Each unit of sol, sip and bel is divided into 11 parts, 1 part is 1/11th unit of noise. The base of logarithm used in noise measurement equations is 11. Table 7 has summarized units of noise and their limiting conditions. Table 8 has provided noise calculation charts.
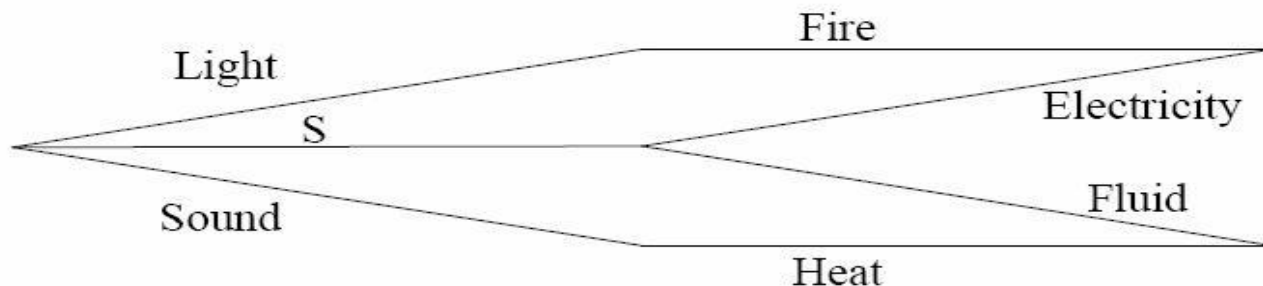

Fig. 5 A Double-Sided Hexagonal Scales of Noise with Seven Edges (S denotes Sun)

Table 7   Noise Grades and Flag Colors under Limiting Conditions

Grades	Noise Grades and Flag Colors under Limiting Conditions		
	Noise of Sol	*Noise of Scattering*	*Noise of Elasticity*
$G_2{}^a$ = ±U	Sol	Sip	Bel
G_1 = G_2 = U	No Positive Solar Energy	No Positive Fluid Energy	No Positive Sound Energy
Base Color for G_1 = G_2			
G_1 = U+→0 Wm^{-2}	Decreasing Solar Energy	Decreasing Fluid Energy	Decreasing Sound Energy
Base Color for G_2			
G_1= + ve	Increasing Solar Energy	Increasing Fluid Energy	Increasing Sound Energy
Base Color for G_2			
G_1 = -U Wm^{-2}	Negative Solar Energy	Negative Fluid Energy	Negative Sound Energy
	Darkness	Low Pressure	Inaudible range
Base Color for G_2			
G_1 = -ve	Darkness increasing, distance from point source of light increasing	Low pressure increasing, vacuum approaching	Inaudible range increasing, vacuum approaching
Base Color for G_2			
G_1 = -U+→0 Wm^{-2}	Negative Solar Energy	Negative Fluid Energy	Negative Sound Energy
	Decreasing Darkness	Decreasing Low Pressure	Decreasing inaudible range
Base Color for G_2			

a. Reference value of G_2 = ±U signifies the limiting condition with areas of noise interference approaching to zero.

---

* Himanshu Dehra (Corresponding author): anshu_dehra@hotmail.com

Table 8 Noise calculation chart estimating onci Sol, onci Sip and onci Bel

a	b	Intensity Ratio (11^a)	Pressure Ratio (11^b)	←oSol→ ←oSip→ ←oBel→	Pressure Ratio $(1/11)^b$	Intensity Ratio $(1/11)^a$
0	0	1	1	0	1	1
1/11	1/22	1.244	1.115	± 01	0.897	0.804
2/11	2/22	1.546	1.244	± 02	0.804	0.647
4/11	4/22	2.392	1.546	± 04	0.647	0.418
6/11	6/22	3.699	1.923	± 06	0.520	0.270
8/11	8/22	5.720	2.392	± 08	0.418	0.175
10/11	10/22	8.845	2.974	± 10	0.336	0.113
12/11	12/22	13.679	3.699	± 12	0.270	0.073
14/11	14/22	21.155	4.599	± 14	0.217	0.047
16/11	16/22	32.715	5.720	± 16	0.175	0.031
18/11	18/22	50.594	7.113	± 18	0.141	0.020
20/11	20/22	78.242	8.845	± 20	0.113	0.013
22/11	22/22	121.000	11.000	± 22	0.091	8.264×10^{-3}
24/11	24/22	187.124	13.679	± 24	0.073	5.344×10^{-3}
26/11	26/22	289.383	17.011	± 26	0.059	3.456×10^{-3}
28/11	28/22	447.525	21.155	± 28	0.047	2.235×10^{-3}
30/11	30/22	692.089	26.308	± 30	0.038	1.445×10^{-3}
32/11	32/22	1070	32.715	± 32	0.031	9.343×10^{-4}
34/11	34/22	1655	40.684	± 34	0.025	6.042×10^{-4}
36/11	36/22	2560	50.594	± 36	0.020	3.907×10^{-4}
38/11	38/22	3959	62.917	± 38	0.016	2.526×10^{-4}
40/11	40/22	6122	78.242	± 40	0.013	1.633×10^{-4}
42/11	42/22	9467	97.300	± 42	0.010	1.056×10^{-4}
44/11	44/22	14640	121.0	± 44	8.264×10^{-3}	6.830×10^{-5}
46/11	46/22	22640	150.47	± 46	6.646×10^{-3}	4.417×10^{-5}
48/11	48/22	35020	187.12	± 48	5.344×10^{-3}	2.856×10^{-5}
50/11	50/22	54150	232.70	± 50	4.297×10^{-3}	1.847×10^{-5}
66/11	66/22	1.772×10^6	1331	± 66	7.513×10^{-4}	5.645×10^{-7}
77/11	77/22	1.949×10^7	4414	± 77	2.265×10^{-4}	5.132×10^{-8}
88/11	88/22	2.144×10^8	14640	± 88	6.830×10^{-5}	4.665×10^{-9}
99/11	99/22	2.358×10^9	48560	± 99	2.059×10^{-5}	4.241×10^{-10}
110/11	110/22	2.594×10^{10}	161100	± 110	6.209×10^{-6}	3.855×10^{-11}

Example: To find oSol corresponding to a pressure ratio of 363
Ratio of 363 = 11X33
In oSol = +22+32 oSol
　　　= +**54 oSol**